Available online at www.sciencedirect.com
ScienceDirect
Polymer 49 (2008) 1701–1715
polymer
www.elsevier.com/locate/polymer

Position and orientation distributions for locally self-avoiding walks in the presence of obstacles

Aris Skliros, Gregory S. Chirikjian*

Department of Mechanical Engineering, Johns Hopkins University, 3400 North Charles Street, Baltimore, MD 21218, USA

Received 1 September 2007; received in revised form 21 January 2008; accepted 23 January 2008
Available online 1 February 2008

Abstract

This paper presents a new approach to study the statistics of lattice random walks in the presence of obstacles and local self-avoidance constraints (excluded volume). By excluding sequentially local interactions within a window that slides along the chain, we obtain an upper bound on the number of self-avoiding walks (SAWs) that terminate at each possible position and orientation. Furthermore we develop a technique to include the effects of obstacles. Thus our model is a more realistic approximation of a polymer chain than that of a simple lattice random walk, and it is more computationally tractable than enumeration of obstacle-avoiding SAWs. Our approach is based on the method of the lattice motion-group convolution. We develop these techniques theoretically and present numerical results for 2-D and 3-D lattices (square, hexagonal, cubic and tetrahedral/diamond). We present numerical results that show how the connectivity constant μ changes with the length of each self-avoiding window and the total length of the chain. Quantities such as $\langle R \rangle$ and others such as the probability of ring closure are calculated and compared with results obtained in the literature for the simple random walk case.

Keywords: Locally self-avoiding walks; Excluded volumes; Obstacles

1. Introduction and literature review

We define an *L-locally self-avoiding walk* to be a random walk of length N in which every subsegment of the walk of a fixed size $L < N$ contains no self-intersections. In principle, given a collection of random walks of length N, those that are L-locally self-avoiding could be extracted by sliding a window of length L along the length of each walk, and removing each walk from the collection if it has at least one self-intersection within any such window. Of course, this would be an exponentially complex calculation due to the cost of enumerating random walks. In contrast, what is presented here is an algorithm for finding the distribution of end positions and orientations for all L-locally self-avoiding walks of length N in an algorithm that has polynomial complexity in N for each fixed L.

L-locally self-avoiding walks differ from other concepts presented in the literature, and are motivated by the observation that polypeptide chains in the unfolded state have steric interactions that reach more than from residue i to $i+1$ [1]. In what follows, we make a distinction between several concepts presented in the literature: random walks (RWs), non-reversal random walks (NRRWs), torsional random walks (TRWs), self-avoiding walks (SAWs), and the locally self-avoiding walks (LSAWs) defined here. For example in the cubic lattice a random walk can move in six directions. The NRRW model will allow five directions (all but the direction pointing backwards along the direction of the current move). The TRW model would allow only four directions (those which are orthogonal to the direction of the current move) [45]. The distinction between NRRW and torsional models is really only important for square and cubic lattices, since there is no way for consecutive bonds to be parallel in the hexagonal and tetrahedral lattices. If the number of rotational moves available around each bond vector is z, then the total number of conformations that can be generated by a torsional random

* Corresponding author. Tel.: +1 4105 167127.
E-mail addresses: askliro1@jhu.edu (A. Skliros), gregc@jhu.edu (G.S. Chirikjian).

0032-3861/$ - see front matter © 2008 Elsevier Ltd. All rights reserved.
doi:10.1016/j.polymer.2008.01.056

walk model is z^n [58]. LSAWs restrict the allowable moves further (though not as much as SAWs when $L < N$), and as $L \to N$, the LSAWs become SAWs.

Consider an ensemble of all possible L-locally self-avoiding random walks, each of length N, in a D-dimensional lattice with obstacles. Under some solvent conditions this can be a more realistic model of a serial polymer (or polypeptide chain) than classical Gaussian or unconstrained random walk models. Furthermore, it is more tractable than the enumeration of all self-avoiding walks. The ability to incorporate local self-avoidance and global obstacle constraints in a computationally tractable framework represents a new step in the direction of using polymer models to describe biomolecular processes in living cells.

For the past fifty years Polymer Theory has used random and self-avoiding walks on lattices extensively. Given the structure of a polymer molecule (consisting of many monomers which have C as their central atom), we can approximate the central atoms as lattice sites and the covalent bonds as lattice edges. Since the quantity $\mathbf{r}_{i-1}$ stands for the position of the ith lattice site of the random walk, then the bond vector, $\mathbf{b}_i = \mathbf{r}_i - \mathbf{r}_{i-1}$, connects two central carbon atoms of sequential monomers. By summing the N bond vectors of $N+1$ identical monomers in the chain we find the end-to-end distance vector $\mathbf{r}$ [20]:

$$\mathbf{r} = \sum_{i=1}^{N+1} \mathbf{r}_i - \mathbf{r}_{i-1}. \tag{1}$$

The corresponding end-to-end distance is $R = |\mathbf{r}|$. The mean square of the latter $\langle R^2 \rangle$ is a very important entity for characterizing the structure of the polymer [20,4]. Other important physical quantities are related to the distribution of values of R, denoted here as $p_N(R)$ for a chain of length N. A multitude of simulation methods has been developed to obtain information about how $p_N(R)$ evolves for polymer chains [10–12]. These methods have been applied to many models of polymer chains. Many researchers resort to the use of lattice random walk models to estimate $\langle R^2 \rangle$. Random walks on lattices with an excluded volume is a more realistic approach than simple random walks on lattices and it has been thoroughly studied too [3,6,7,21,59,60].

Self-avoiding walks is a topic on which many papers like Refs. [25,29,30,33–36,39] and books have been written. A classic book on this topic is by Madras and Slade [13]. It is believed that the number of self-avoiding walks on any lattice increases exponentially as the number of segments increases [13]. The limiting behavior for large values of N is described by the *connectivity constant* defined as

$$\mu = \lim_{N \to \infty} c_N^{1/N}.$$

This equation simply says that the connectivity constant, for the random walks of N segments is defined by the Nth root of C_N, the number of self-avoiding walks of N segments.

The number of self-avoiding walks has been enumerated for up to a fixed number of segments for the square lattice (up to 71) [50,18], the hexagonal lattice [46,54] (up to 48), for the cubic lattice [19] (up to 26) and for the tetrahedral (diamond) lattice [47] (up to 30). Previous methods in diamond lattice had counted up to 20 segments and their end-to-end length distributions using a counting theorem [41]. Other methods in diamond lattice SAWs have extended the excluded volume condition [33]. Some works have exhaustively enumerated SAWs on cubic lattices by either using the Hamiltonian function [14], the Transfer matrix method [16], or other methods [51]. The same method (Transfer matrix) is used to count walks on square lattices [15,26], or in rectangular lattices [27]. Works in the past on the cubic lattice also have studied the asymptotic behavior of the number of self-avoiding walks (c_n) on it [44]. Various other methods have also been presented for counting self-avoiding walks on the square lattice [17,53]. Faulon et al. have proved that n-step self-avoiding walks on the square, tetragonal, cubic and tetrahedral lattices can be uniquely characterized with no more than n-Euclidean distances. Papers have also been written on behavior of the distribution function for self-avoiding walks [24]. Watts has made a study of the mean square lengths of self-avoiding walks on a number of loose-packed lattices [42]. Mathematical techniques such as knot theory have also been used to describe self-avoiding walks on lattices [43,48]. The importance of the study of self-avoiding walks in polymer science is noted in [40,52,49,20,23,28,37,38]. Other papers have worked on self-avoiding walks, on honeycomb lattice by using the chain generating function method [22], on various 2-D and 5-D lattices by exact enumeration by concatenation [32] and on the L-lattice by the re-normalization group approach [31]. Studies on self-avoiding walks have also used Monte-Carlo method to approximate their number [5,8]. Papers have also been written on behavior of the distribution function for self-avoiding walks [24,25]. To our knowledge, no other works have generated statistics on locally self-avoiding walks. In our view, these chains represent a computationally tractable model that combines features of RWs and SAWs.

2. Definitions and formulation

Let the coordination number of the lattice walk be denoted as z. That is, in the absence of obstacles and self-interaction constraints (other than immediate reversals), there are z possible moves that the walk can take at each step. Each move generates a link or bond to the previous position. For polymer models, each value, 1, 2, …, z corresponds to a different value of the torsion/dihedral angle describing rotation of the newest bond around the previous one. The vector of all such angles for a chain of length N is defined as ϕ^N. The set $\{\phi_i^N\}$ for $i = 1, 2, \ldots, z^N$ denotes all possible combinations of angles. When the length of the chain is clear from the context, we will drop the superscript N.

In the absence of obstacles, if we want to 'grow' the statistics of the complete ensemble of all L-locally self-avoiding chains that are planted at the identity frame, we can do this recursively (assuming that L is an even number) as follows.

First, enumerate all self-avoiding walks of length $L/2$. There will be $n(L/2) \leq z^{L/2}$ of these. Here the function $n(l)$ denotes the number of SAWs of length l. Next, join all pairs of these two self-avoiding segments, and construct a $n(L/2) \times n(L/2)$ table

consisting of zeros whenever there is at least one intersection between segment 1 and segment 2. This table can be denoted as $W(\phi', \phi)$, where ϕ' is the $L/2$-dimensional vector of torsion angles of the proximal part of the chain, and ϕ is the $L/2$-dimensional vector of torsion angles of the distal part of the chain.

Explicitly, we let $g(\phi_i^m)$ denote the forward kinematic function that produces the end position and orientation of a chain of length m defined by torsion angles ϕ_i^m. In the notation of homogeneous transformations [45],

$$g = \begin{pmatrix} A & \mathbf{r} \\ 0^{\mathrm{T}} & 1 \end{pmatrix}, \tag{2}$$

and two rigid body motions compose as $g_1 \circ g_2$, which is performed as matrix multiplication. The same position and orientation can be reached by different possible joint angles. In other words, it is possible for $g(\phi_i) = g(\phi_j)$ even though $i \neq j$.

The position (or translation) and orientation (or rotation) can be extracted from g by defining $\mathbf{r}[g] = \mathbf{r}$ and $A[g] = A$, respectively. Therefore, in this notation

$$A[g_1 \circ g_2] = A_1 A_2 = A[g_1]A[g_2]$$

and

$$\mathbf{r}[g_1 \circ g_2] = A_1 \mathbf{r}_2 + \mathbf{r}_1 = A[g_1]\mathbf{r}[g_2] + \mathbf{r}[g_1].$$

The set of all values of g together with the composition operation, $\circ$, in our context forms a proper crystallographic space group (where "proper" means that $\det(A) = +1$ so that reflections are excluded). We also call this a *lattice motion group*, and denote it as G. Any $g \in G$ can act on a lattice point $x \in \mathbb{L}$ according to the rule:

$$g \cdot x = Ax + \mathbf{r}.$$

In practice, we are only concerned with a finite subset of G, since a chain of length N consisting of links with unit lengths will always be contained within a ball of radius N from its starting point.

In the simplest possible case, when one does not care about local (or global) self-avoidance or obstacles, the statistics for long chains can be generated from those of shorter chains by convolution [45]. In particular, if we seek to generate the number distribution of end position and orientation for a chain of length $N + L/2$ from those of length N and length $L/2$, we perform the convolution [45]:

$$f_{N+L/2}(g) = \sum_{h \in G} f_N(h) f_{L/2}\left(h^{-1} \circ g\right). \tag{3}$$

The reason for performing such convolutions, as opposed to purely translational convolutions in the lattice, is that the accessible moves when traversing each bond has a different appearance in a frame of reference fixed to the bond, and a frame of reference fixed in space. For example, the set of one-step moves available to a non-reversal random walk is a constant set in the reference frame attached to the distal bond. However, in the space-fixed frame the directions of allowable moves depend on the orientation of the bond-fixed frame. Eq. (3) does not take into account local self-interactions of the chain. All conformations, both self-avoiding and self intersecting, are generated.

Returning to the locally self-avoiding case, and using this notation, we have for each $I, J \in \{1, 2, \ldots, n(L/2)\}$

$$W\left(\phi_I'^{\,L/2}, \phi_J^{L/2}\right) = 0 \text{ if } \mathbf{r}\left[g\left(\phi_I'^{\,L/2}\right) \circ g\left(\phi_J^j\right)\right] = \mathbf{r}\left[g\left(\phi_I'^{\,i}\right)\right]$$

for any $i, j \in \{1, 2, \ldots, L/2\}$. Similarly, if any part of the second segment intersects the first, this constitutes a self-intersection of the concatenated chain. Therefore, for each $I, J \in \{1, 2, \ldots, n(L/2)\}$

$$W\left(\phi_I'^{\,L/2}, \phi_J^{L/2}\right) = 0 \quad \text{if } \mathbf{r}\left[g\left(\phi_I'^{\,L/2}\right) \circ g\left(\phi_J^j\right)\right] = 0$$

for any $j \in \{1, 2, \ldots, L/2\}$.

If neither of the above conditions holds, $W(\phi_I', \phi_J) = 1$.

Our assumption is that $L/2$ is a number small enough (for example, 2,4,6 or 8) that it is possible to compute and store $W(\phi', \phi)$ and enumerate all values of $g(\phi^{L/2})$. In fact, our assumption is that $L/2$ is small enough that it would be no problem to *store* the array containing the number density function describing the frequency of occurrence of the joint information of position and orientation and the distal $L/2$ joint angles. This number density is denoted as $f_N(g, \phi^{L/2})$.

3. Recursive generation of position and orientation and torsion angle distributions for locally self-avoiding walks

The joint number distribution of position and orientation and torsion angles for a self-avoiding segment of length $L/2$ is computed by basically counting:

$$f_{L/2}(g', \phi) = \delta\left([g(\phi)]^{-1} \circ g'\right), \tag{4}$$

where g' is an arbitrary position and orientation and the dimension of all vectors ϕ are $L/2$. When summing over ϕ it will henceforth be understood that we are summing over all individual values.

In Fig. 1 we see a random walk of length N to which a random walk of length $L/2$ is pasted at the distal end. Fig. 1 shows the result of this concatenation for various cases including the presence of obstacles. In the case that the $N + L/2$ walk terminates somewhere in the $L/2$-length distal end of the N length walk or inside the obstacle then the walk is discarded. Discarded walks are drawn by dotted-darker line.

In the absence of obstacles, we can obtain the distribution $f_{N+L/2}(g, \phi^{L/2})$ from $f_N(g', \phi^{L/2})$ and $f_{L/2}(g', \phi^{L/2})$ by computing:

$$f_{N+L/2}(g', \phi) = \sum_{\phi'} \sum_{h \in G} f_N(h, \phi') W(\phi', \phi) f_{L/2}\left(h^{-1} \circ g', \phi\right), \tag{5}$$

where the dimensions of all vectors ϕ and ϕ' are both $L/2$.

In other words, we can extend the walk by length $L/2$ by convolving the distribution of end positions and orientations for the segment of length $L/2$ with that of length N, and

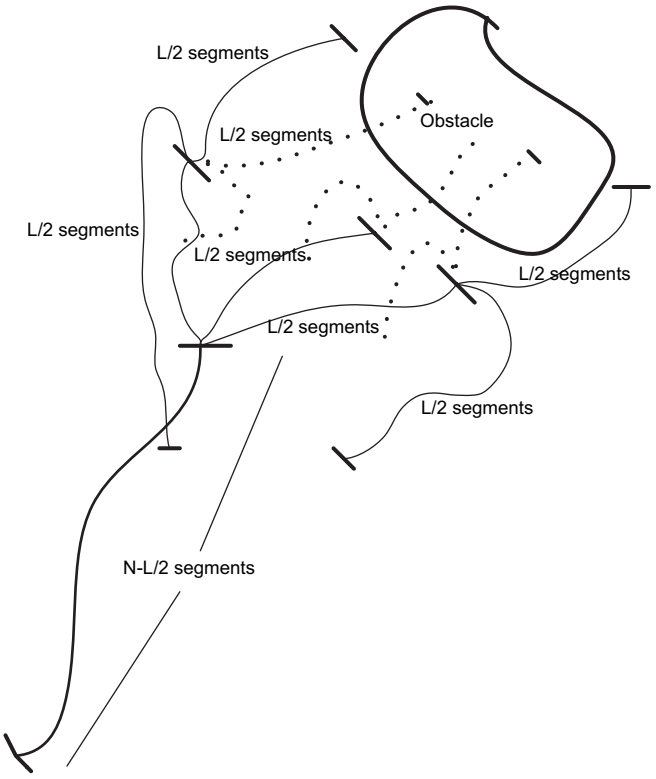

Fig. 1. A random walk of length N to which a random walk of length $L/2$ is pasted at the distal end. In the case that the $N+L/2$ walk terminates somewhere in the $L/2$-length distal end of the N length walk or inside the obstacle then the walk is discarded. Discarded walks are drawn by dotted-darker line.

enforce the property that none of the newly added walks intersect the distal $L/2$ links of the walks of length N.

Substituting Eq. (4) into Eq. (5), we see that

$$\begin{aligned} f_{N+L/2}(g',\phi) &= \sum_{\phi'}\sum_{h\in G} f_N(h,\phi')W(\phi',\phi)\left[\delta\left([g(\phi)]^{-1}\circ h^{-1}\circ g'\right)\right] \\ &= \sum_{\phi'} W(\phi',\phi)\left[\sum_{h\in G} f_N(h,\phi')\delta\left([g(\phi)]^{-1}\circ h^{-1}\circ g'\right)\right] \\ &= \sum_{\phi'} f_N\left(g'\circ[g(\phi)]^{-1},\phi'\right)W(\phi',\phi). \end{aligned}$$

The reason for this simplification is that the delta function kills all entries in the summation over $h\in G$ except $[g(\phi)]^{-1}\circ h^{-1}\circ g' = e$, which means that the only h that survives is $h^{-1} = g(\phi)\circ(g')^{-1}$, or $h = g'\circ[g(\phi)]^{-1}$.

In short then, we have the following formula that can be applied recursively to compute the joint distribution of end position and orientation and the distal $L/2$ torsion angles:

$$f_{N+L/2}(g',\phi) = \sum_{\phi'} f_N\left(g'\circ[g(\phi)]^{-1},\phi'\right)W(\phi',\phi). \tag{6}$$

Note that there is no sum over G remaining. This is an upper bound on the number of self-avoiding walks of length N. As L becomes larger, this bound becomes tighter.

4. How to handle obstacles

An obstacle in a D-dimensional lattice can be characterized by a cloud of lattice points through which a random walk is not allowed to pass. It is sufficient to only consider the points on the exterior of such a cloud, since if a walk cannot occupy exterior points of the obstacle, then it cannot penetrate into the interior. The number of points on the surface of a large convex obstacle in a D-dimensional lattice will be significantly smaller than the total number of obstacle points. Therefore, we only enumerate such surface/exterior points when describing an obstacle.

4.1. Obstacles without self-avoiding constraints

We begin by addressing how to handle statistics of walks *without local self-avoidance constraints* in the presence of obstacles. In order to be consistent with the formulation of the prior section, for eventual merger of the results from that section with this one, we will grow chain statistics by a length of $L/2$ on each recursion similar to what is done in Eq. (3). Let us assume that $f_N(g)$ is the number distribution of position and orientation for a random walk of length N that avoids obstacles defined by a set of lattice points $\{\mathbf{o}_k\}$ the total number of such points in $|\{\mathbf{o}_k\}| = K$, and that this distribution has been precalculated (by whatever means). Now suppose that we want to 'extend' these walks by length $L/2$ by 'attaching' the walk distribution $f_{L/2}(g)$ (which has no obstacle-avoiding properties) to the ends of the current walk, and then account for intersections with the obstacles. In the case when $L/2 = 1$, this was done very simply in Refs. [2,45] by performing the basic convolutions in Eq. (3), and then after each convolution zeroing any nonzero density on the interior of the obstacle. The trouble is that this approach does not work when extending by a length $L/2 > 1$, because the distal end of the walk has enough freedom to then enter the obstacle with its penultimate vertex, and still place the most distal vertex outside the obstacle. Therefore, the extension of Eq. (3) to the case when obstacles are present must account for, and subtract, contributions that lead to intersections with obstacles *before* adding the contributions of each extension into $f_{N+L/2}(g)$.

In order to do this, we first recall that $f_{L/2}(g)$ can be rewritten as in Eq. (4) when there are no obstacles. Each ϕ describes one walk of length $L/2$. If any part of this walk intersects any part of an obstacle, then this whole walk (and, specifically, its corresponding end position and orientation) must be 'removed' from $f_{L/2}(g)$. The difficulty is that the walks that should be removed depend on how the collection of walks summarized in $f_{L/2}(g)$ has been moved. In short then, we modify $f_{L/2}(h^{-1}\circ g')$ in Eq. (5) as:

$$\begin{aligned} f_{L/2}\left(h^{-1}\circ g'\right) = \sum_{\phi}\delta\left([g(\phi)]^{-1}\circ h^{-1}\circ g'\right)\prod_{k=1}^{K}\prod_{j=1}^{L/2} \\ \left[1-\delta\left(h\cdot\mathbf{r}\left[g\left(\phi_j^l\right)\right]-\mathbf{o}_k\right)\right], \end{aligned} \tag{7}$$

where $\mathbf{r}[g(\phi_j^l)]$ is the position of the j^{th} point ($j < L/2$) along the chain defined by the set of $L/2$ torsion angles ϕ. The expression $\delta(h\cdot\mathbf{r}[g(\phi_j^l)]-\mathbf{o}_k)$ is equal to zero when $h\cdot\mathbf{r}[g(\phi_j^l)]\neq\mathbf{o}_k$ (in which case one minus this is equal to one, and the walk is not disallowed). However, when $h\cdot\mathbf{r}[g(\phi_j^l)] = \mathbf{o}_k$, the delta function is equal to one, which means that one minus one gives zero. Since the above are all multiplied, if any of the terms $[1-\delta(h\cdot\mathbf{r}[g(\phi_j^l)]-\mathbf{o}_k)]$ is zero, the whole product is killed. If several intersections of one walk with the obstacle occur, this is not double counted since it will only result in several multiplications by the number zero.

Basically, Eq. (7) says that as we rigidly move $f_{L/2}(g)$ around (i.e., shift from the left by h^{-1}), we remove all contributions to it from all chains that have any part that intersects any obstacle point.

The modified convolution to account for obstacles then takes the form:

$$\begin{aligned} f_{N+L/2}(g') &= \sum_{h\in G} f_N(h)\left[\sum_{\phi}\delta\left([g(\phi)]^{-1}\circ h^{-1}\circ g'\right)\right. \\ &\quad\left.\times\prod_{k=1}^{K}\prod_{j=1}^{L/2}\left[1-\delta\left(h\cdot\mathbf{r}\left[g\left(\phi^j\right)\right]-\mathbf{o}_k\right)\right]\right] \\ &= \sum_{\phi} f_N\left(g'\circ[g(\phi)]^{-1}\right)\prod_{k=1}^{K}\prod_{j=1}^{L/2} \\ &\quad\times\left[1-\delta\left(g'\circ[g(\phi)]^{-1}\cdot\mathbf{r}\left[g\left(\phi^j\right)\right]-\mathbf{o}_k\right)\right], \end{aligned} \tag{8}$$

where the same calculation with the delta function that resulted in Eq. (6) has been performed.

4.2. Combining obstacle effects and local self-avoidance

We can now simply combine the results in the two prior sections to generate the joint distribution of end position and orientation and distal torsion angles for L-locally self-avoiding walks in the presence of obstacles:

$$\begin{aligned} f_{N+L/2}(g',\phi) &= \sum_{\phi'}\sum_{h\in G} f_N(h,\phi')W(\phi',\phi)\left[\delta\left([g(\phi)]^{-1}\circ h^{-1}\circ g'\right)\right. \\ &\quad\left.\times\prod_{k=1}^{K}\prod_{j=1}^{L/2}\left[1-\delta\left(h\cdot\mathbf{r}\left[g\left(\phi^j\right)\right]-\mathbf{o}_k\right)\right]\right] \\ &= \sum_{\phi'} W(\phi',\phi)\left[\sum_{h\in G} f_N(h,\phi')\delta\left([g(\phi)]^{-1}\circ h^{-1}\circ g'\right)\right. \\ &\quad\left.\times\prod_{k=1}^{K}\prod_{j=1}^{L/2}\left[1-\delta\left(h\cdot\mathbf{r}\left(\left[g\left(\phi^j\right)\right]\right)-\mathbf{o}_k\right)\right]\right] \\ &= \sum_{\phi'} f_N\left(g'\circ[g(\phi)]^{-1},\phi'\right)W(\phi',\phi) \\ &\quad\times\prod_{k=1}^{K}\prod_{j=1}^{L/2}\left[1-\delta\left(g'\circ[g(\phi)]^{-1}\cdot\mathbf{r}\left[g\left(\phi^j\right)\right]-\mathbf{o}_k\right)\right]. \end{aligned}$$

4.3. Special treatment for the tetrahedral lattice

The tetrahedral lattice differs from others in that it is "two-definable" [61]. This means that walks of even and odd lengths are treated differently. As shown in Refs. [45,2] for finding $f_{N+L/2}(g')$ we modify Eq. (3) as:

$$f_{N+L/2}(g') = \sum_{h\in G} f_N(h) f_{L/2}\left(A_h^{\mathrm{T}}A_{g'}, \pm A_h^{\mathrm{T}}\left(\chi_{g'}-\chi_h\right)\right) \tag{9}$$

given that $h=(A_h,\chi_h)$, $g'=(A_{g'},\chi_{g'})$ representing orientations and positions depending on whether N is even or odd number, respectively. Now the analog of having $\delta([g(\phi)]^{-1}\circ h^{-1}\circ g') = 1$ in the case where N is odd is derived by solving the following equation:

$$\begin{bmatrix} A_{g(\phi)} & \chi_{g(\phi)} \\ 0^{\mathrm{T}} & 1 \end{bmatrix} = \begin{bmatrix} A_h^{\mathrm{T}}A_{g'} & -A_h^{\mathrm{T}}\left(\chi_{g'}-\chi_h\right) \\ 0^{\mathrm{T}} & 1 \end{bmatrix}. \tag{10}$$

5. Computational cost and numerical results

5.1. Computational cost

Before computing analytically the computational cost for the local interactions for the obstacle case and for the combinations of local interactions with obstacles we need first to define some quantities. N_t is the target number of segments we want to reach with the recursion method. $n(L/2)$ is number of self-avoiding walks of length $L/2$, $(N+L/2)^D$ is the order of the number of positional entries in an array for the updated chain of length $N+L/2$ in a D-dimensional lattice, and $|\mathbb{P}|$ is the number of rotational elements in the proper point group of the lattice. Finally $|K|$ is the number of obstacle points. The cost of one recursion of Eq. (6) is $O([n(L/2)]^2\cdot(N+L/2)^D\cdot|\mathbb{P}|)$. The cost of one recursion of Eq. (8) is $O([n(L/2)]\cdot(N+L/2)^D\cdot|\mathbb{P}|\cdot|K|)$. The cost of one recursion of Eq. (9) is $O([n(L/2)]^2\cdot(N+L/2)^D\cdot|\mathbb{P}|\cdot|K|)$. The cost for multiple recursions of Eq. (6) is

$$\sum_{N=L/2}^{N_t} O\left([n(L/2)]^2\cdot(N+L/2)^D\cdot\left|\mathbb{P}\right|\right),$$

where the step of the summation is $L/2$. The cost of multiple recursions of Eq. (8) is

$$\sum_{N=L/2}^{N_t} O\left([n(L/2)]\cdot(N+L/2)^D\cdot\left|\mathbb{P}\right|\cdot\left|K\right|\right).$$

The cost of multiple recursions of Eq. (9) is

$$\sum_{N=L/2}^{N_t} O\left([n(L/2)]^2\cdot(N+L/2)^D\cdot\left|\mathbb{P}\right|\cdot\left|K\right|\right).$$

The computational costs for these three foregoing multiple recursions are $O(N^{D+1})$. The quantities $|\mathbb{P}|$ and $|K|$ serve as constants. We see that things go much faster, that is, the computational cost is $O(N^{D+1})$. We have implemented

the above method for $L = 4$ for the square and for $L = 6$ for the hexagonal lattice. This is because the first self-intersections in these lattices occur at $N = 4$, $N = 6$, respectively, where N is the number of segments of the random walk. Furthermore since our goal is to demonstrate the method with some numerical results and since the computational cost is a strictly increasing function of L we restricted ourselves to the smallest number of L.

5.2. Numerical results

Before proceeding to the presentation of the numerical results we need to specify that ratio8 stands for $\langle R\rangle^8/\langle R^2\rangle^4$, where $\langle R^2\rangle$ is the mean square end-to-end distance. For all the lattices and for all the cases we calculate and present plots for the mean end-to-end distance $\langle R\rangle$, ratio8 and probability of ring closure with respect to N. For the square and hexagonal lattices we also present the distribution of distances for N_t segments. Furthermore, when local interactions are involved we present μ w.r.t. N. Finally for both the planar lattices we present a figure which shows on the lattice the density of walks to each lattice site and from there we can conclude that our method avoids the obstacle because all the lattice sites in the obstacle are unoccupied. The obstacle that was used for the planar lattices is a circle of radius 5 and of center $K = (10,15)$. For the 3-D lattices the obstacles are 12 points selected randomly.

5.2.1. Square lattice

Figs. 2 and 3 show the distribution of walks for the 100 segments random walk on the square lattice when there exists the obstacle and we exclude local interactions. We see the interior of the obstacle is unoccupied.

In Fig. 4 we compare the probability distributions of the distances that are reached by the 100 segment random walk on the square lattice when we exclude obstacles (circles), when we exclude local interactions (dots), when we exclude both local interactions and obstacles (×s) and that of the simple random walk (squares).

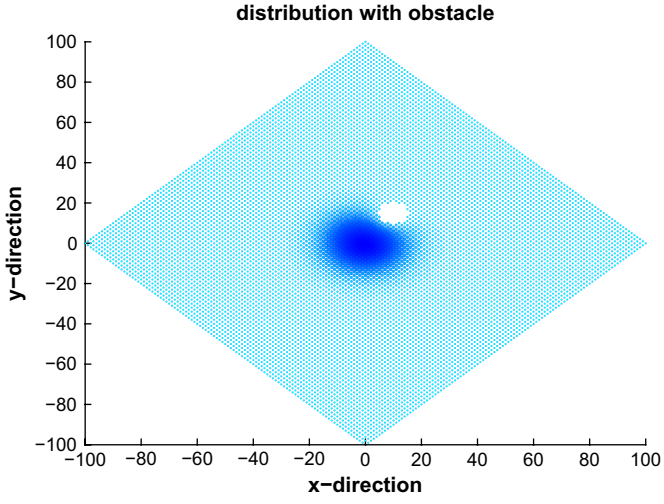

Fig. 2. The distribution of walks for the 100 segments random walk on the square lattice when there exists the obstacle and we exclude local interactions. We see again the interior of the obstacle is unoccupied.

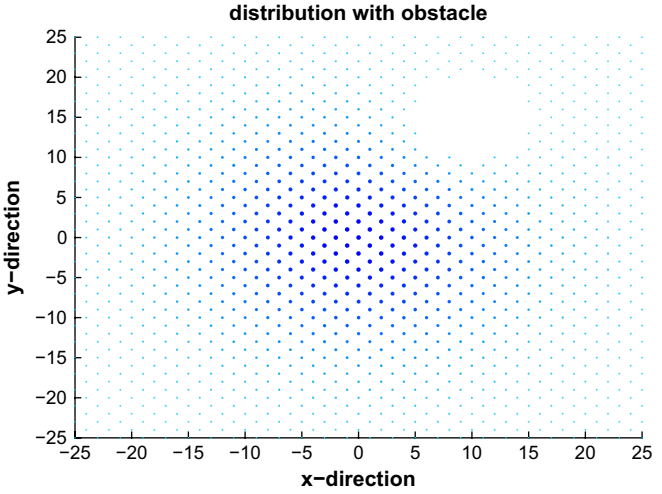

Fig. 3. Zoom in of the figure of square random walks with obstacle and local interactions.

In Fig. 5 we compare the mean end-to-end distance as it evolves as the number of segments increases, of the random walk on the square lattice when we exclude obstacles (circles), when we exclude local interactions (dots), when we exclude both local interactions and obstacles (×s) and the case of the simple random walk (squares).

In Fig. 6 we compare μ as a function of the number of segments for random walks on the square lattice when we exclude local interactions (dots), when we exclude local interactions and obstacles (×s) and we compare it with the line derived by the calculation of μ according to the real number of SAWs (squares) as obtained from the literature [50]. As we notice the constant μ is smaller when we exclude local

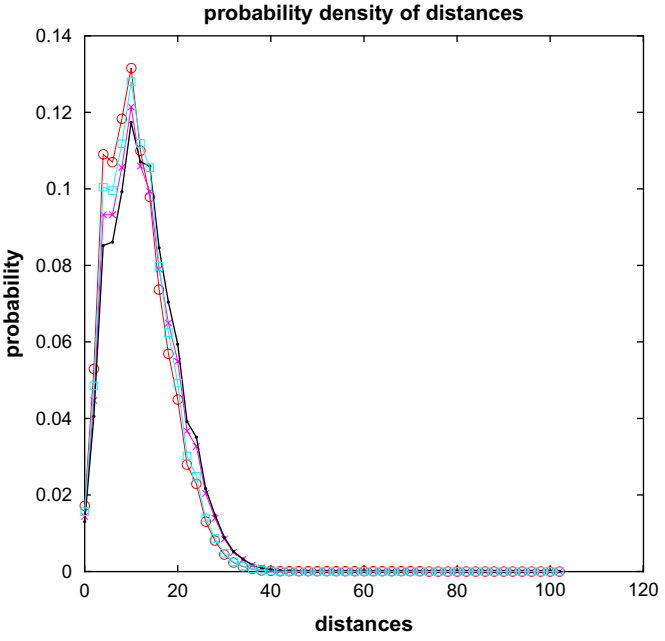

Fig. 4. Comparison of the probability distributions of the distances that are reached by the 100 segment random walk on the square lattice when we exclude obstacles (circles), when we exclude local interactions (dots), when we exclude both local interactions and obstacles (×s) and that of the simple random walk (squares).

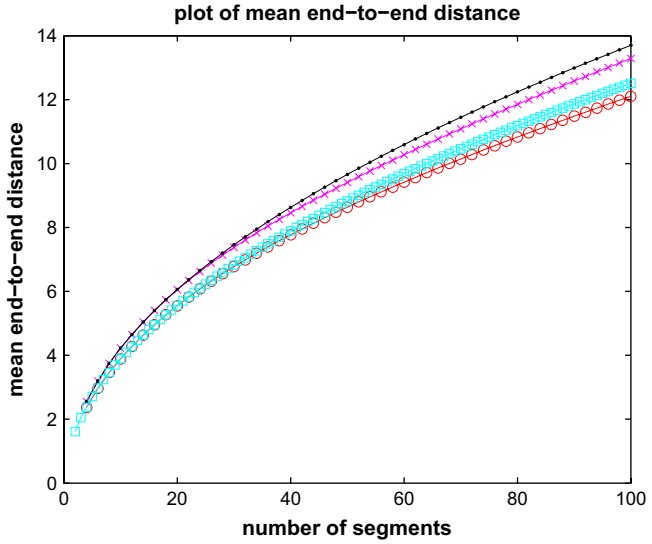

Fig. 5. Comparison of the mean end-to-end distance as it evolves as the number of segments increases, of the random walk on the square lattice when we exclude obstacles (circles), when we exclude local interactions (dots), when we exclude both local interactions and obstacles (×s) and the case of the simple random walk (squares).

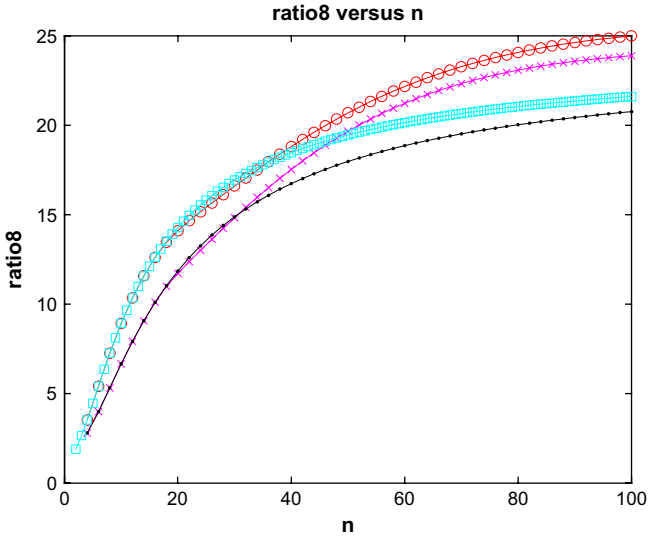

Fig. 7. Ratio8, $\langle R^8\rangle/\langle R^2\rangle^4$, as it evolves as the number of segments increases, of the random walk on the square lattice in the presence of obstacles (circles), when we exclude local interactions (dots), when we exclude both of local interactions and obstacles (×s) and that of the simple random walk as it evolves in the one-step lattice motion-group convolution (squares).

interactions and obstacles than that when we exclude only local interactions. We notice that the upper bounds on the connective constant on the square lattice are much looser even from the results of Noonan and Guttman respectively [56,57] and of course that of the real value of μ for the walks that have been counted (up to 71 segments). Recently in [55] have been presented even tighter approximations. However, our approximation would improve if we took a greater L. That would require an additional computational cost and since our purpose is to demonstrate the development of a method that finds upper bounds in combination with an obstacle we did not consider that necessary.

In Fig. 7 we compare $\langle R^8\rangle/\langle R^2\rangle^4$, as it evolves as the number of segments increases, of the random walk on the square lattice in the presence of obstacles (circles), when we exclude local interactions (dots), when we exclude both of local interactions and obstacles (×s) and that of the simple random walk as it evolves in the one-step lattice motion-group convolution (squares). In Fig. 8 we compare the probability of ring closure

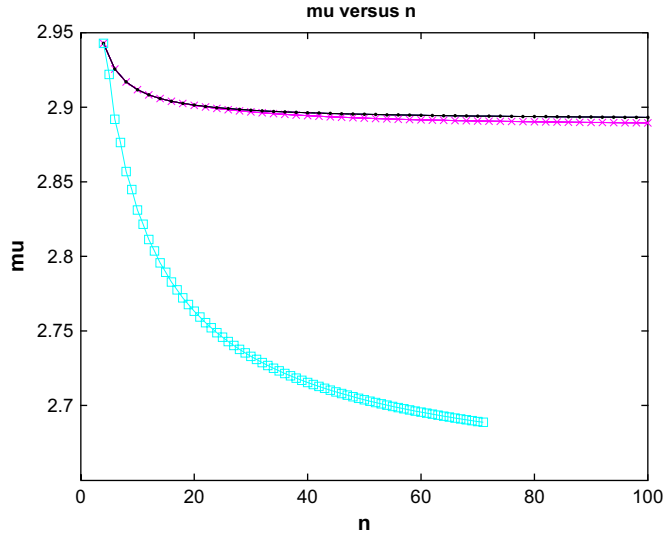

Fig. 6. Comparison of the constant μ as a function of the number of segments for random walks on the square lattice when we exclude local interactions (dots), when we exclude local interactions and obstacles (×s), and line derived by the calculation of μ according to the real number of SAWs (squares) as obtained from the literature.

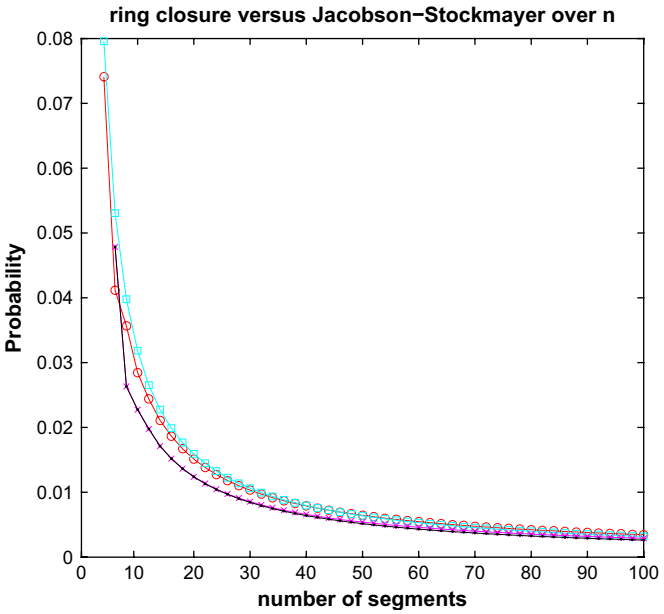

Fig. 8. Comparison of the probability of ring closure (walks terminating at the origin) on the square lattice for the case when we exclude local interactions (dots), when we exclude obstacles (circles), when we exclude both local interactions and obstacles (×s) and that of the 2-D version of the classical Jacobson−Stockmayer result, that is, $P = 1/\pi n$ (squares).

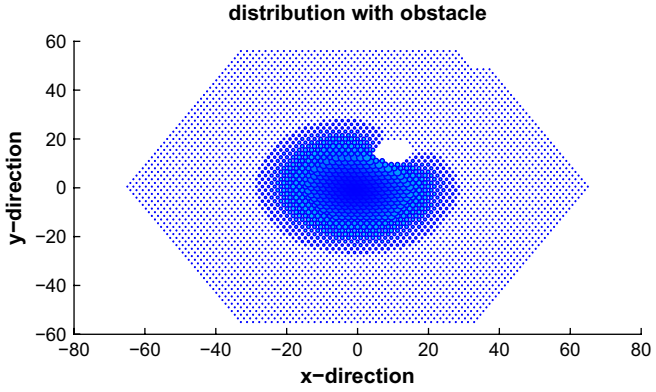

Fig. 9. The distribution of walks for the 75 segments random walk on the hexagonal lattice when there exists the obstacle and we exclude local interactions. The notch is due to the lattice's geometry.

(walks terminating at the origin) for the case when we exclude local interactions (dots), when we exclude obstacles (circles), when we exclude both local interactions and obstacles (×s) and we compare it with the 2-D version of the classical Jacobson–Stockmayer [9] result that is $P = 1/\pi n$ (squares).

5.2.2. Hexagonal lattice

Fig. 9 shows the distribution of walks for the 75 segments random walk on the hexagonal lattice when there exists the obstacle and we exclude local interactions. The notch is due to the lattice's geometry. By a 'notch' we simply mean that there is a location where density is missing, where there would otherwise be density if not for the presence of the obstacle.

In Fig. 10 we compare the probability distributions of the distances that are reached by the 75 segment random walk on the hexagonal lattice in the presence of obstacles (circles), exclusion of local interactions (dots), exclusion of local interactions and obstacles (×s) and the simple random walk (squares). In Fig. 11 we compare the mean end-to-end distance as it evolves as the number of segments increases, of the random walk on the hexagonal lattice in the presence of obstacles (circles), exclusion of local interactions (circles), exclusion of local interactions and obstacles (×s) and the simple random walk (squares).

In Fig. 12 we compare the constant μ, as it evolves as the number of segments increases, of the random walk on the hexagonal lattice when we exclude local interactions (dots) when we exclude local interactions and obstacles (×s) and when we have true number of SAWs obtained in the bibliography (squares). As we notice the constant μ is smaller when we

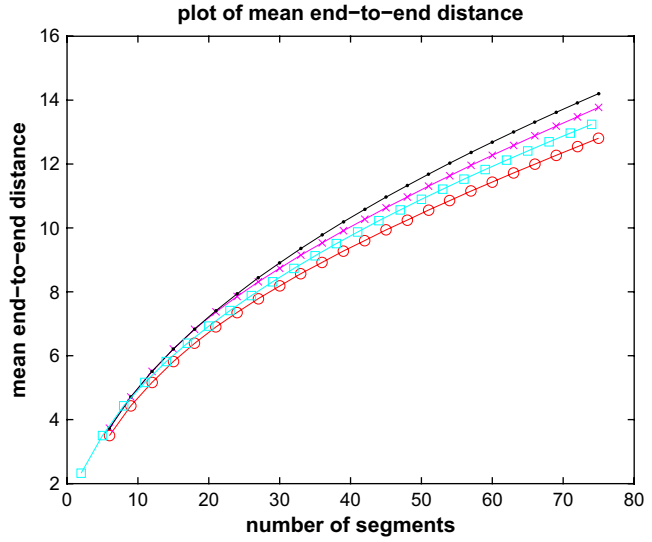

Fig. 11. Comparison of the mean end-to-end distance as it evolves as the number of segments increases, of the random walk on the hexagonal lattice in the presence of obstacles (circles), exclusion of local interactions (circles), exclusion of local interactions and obstacles (×s) and the simple random walk (squares).

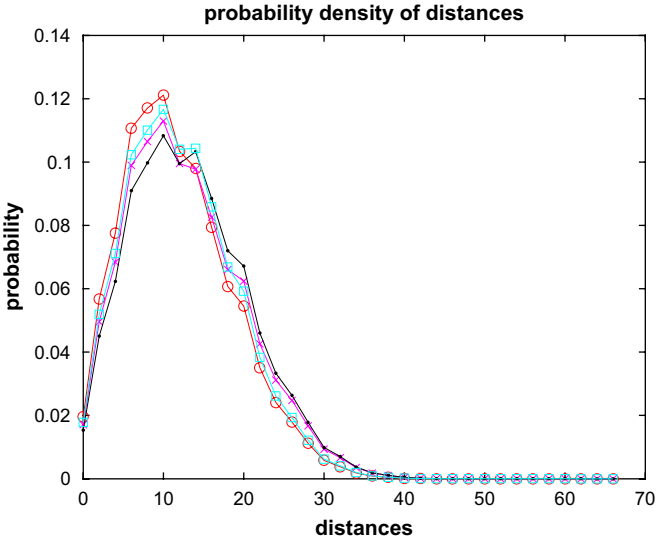

Fig. 10. Comparison of the probability distributions of the distances that are reached by the 75 segment random walk on the hexagonal lattice in the presence of obstacles (circles), exclusion of local interactions (dots), exclusion of local interactions and obstacles (×s) and the simple random walk (squares).

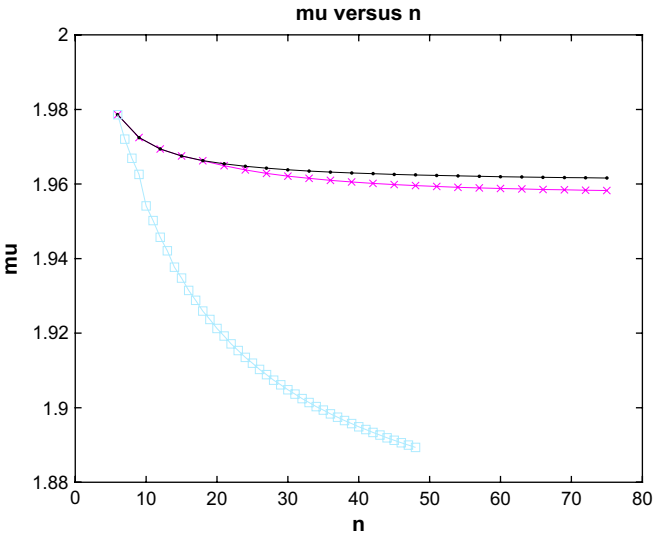

Fig. 12. Comparison of the constant μ, as it evolves as the number of segments increases, of the random walk on the hexagonal lattice when we exclude local interactions (dots), when we exclude local interactions and obstacles (×s) and when we have true number of SAWs obtained in the bibliography (squares).

exclude local interactions and obstacles than that when we exclude only local interactions. We notice that the upper bounds on the connective constant on the hexagonal lattice are much looser from the real value of μ for the walks that have been counted (up to 48 segments). However though, our approximation would be better if we took a greater L. That would require an additional computational cost and since our purpose is to demonstrate the development of a method that finds upper bounds in combination with an obstacle we did not consider that necessary.

In Fig. 13, we compare $\langle R^8\rangle/\langle R^2\rangle^4$, as it evolves as the number of segments increases, of the random walk on the hexagonal lattice in the presence of obstacles (circles), when we exclude local interactions and obstacles (×s) and the simple random walk as it evolves in the one-step lattice motion-group convolution (squares). In Fig. 14 we compare the probability of ring closure (walks terminating at the origin) for the case when we exclude local interactions (dots), when we exclude obstacles (circles), when we exclude both local interactions and obstacles (×s) and we compare it with the 2-D version of the classical Jacobson–Stockmayer [9] result (squares), that is, $P = 1/\pi n$. In the picture we cannot clearly see the line which describes the exclusion of the local interactions because it coincides with the line which describes the exclusion of both local interactions and obstacles.

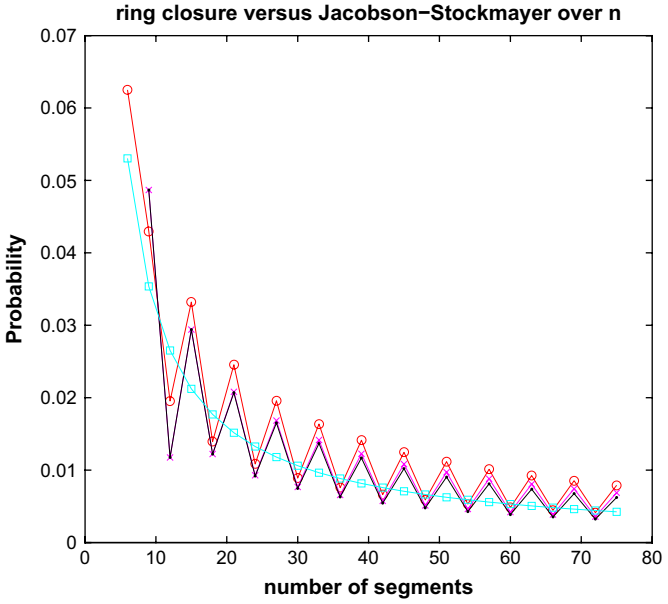

Fig. 14. Comparison of the probability of ring closure on the hexagonal lattice (walks terminating at the origin) for the case when we exclude local interactions (dots), when we exclude obstacles (circles), when we exclude both local interactions and obstacles (×s) and we compare it with the 2-D version of the classical Jacobson–Stockmayer [9] result (squares).

5.3. Cubic lattice

In Fig. 15 we compare the mean end-to-end distance, as it evolves as the number of segments increases, of the random walk on the cubic lattice in the presence of obstacles (circles) and exclusion of local interactions (dots). As we can see from that figure, these quantities diverge in value slightly as the number of segments increase yet the ratio of the values of these two quantities remains constant.

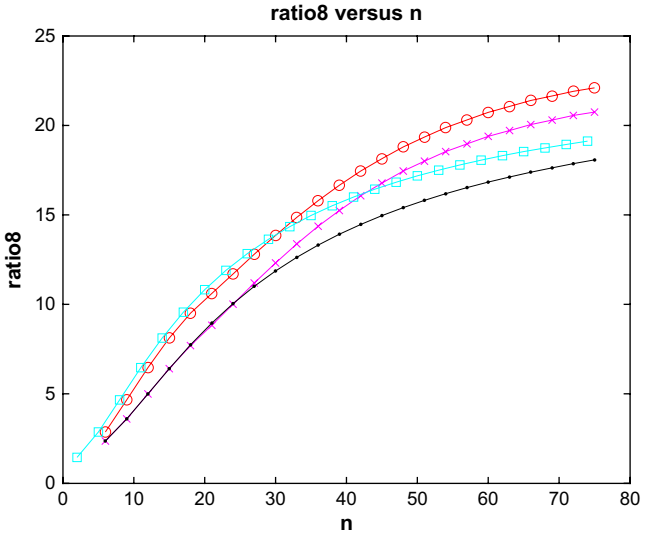

Fig. 13. Ratio8, $\langle R^8\rangle/\langle R^2\rangle^4$, as it evolves as the number of segments increases, of the random walk on the hexagonal lattice in the presence of obstacles (circles), when we exclude local interactions and obstacles (×s) and the simple random walk as it evolves in the one-step lattice motion-group convolution (squares).

In Fig. 16 we compare the constant μ as it evolves as the number of segments increases, of the random walk on the cubic lattice when we exclude the local interactions (dots) with the value of μ as found when we take into account the real number of SAWs (squares). We notice that the upper bounds on the connective constant on the cubic lattice are much looser from the real value of μ for the walks that have been counted (up to 26 segments). However though, our approximation would be better if we took a greater L. That would require an additional computational cost and since our purpose is to demonstrate

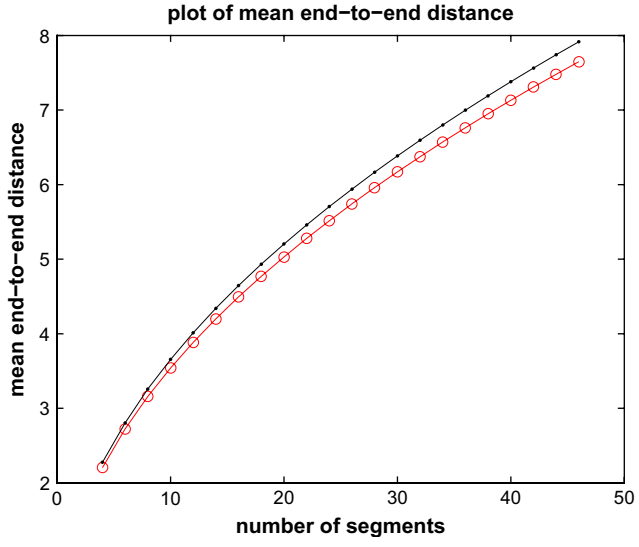

Fig. 15. Comparison of the mean end-to-end distance, as it evolves as the number of segments increases, of the random walk on the cubic lattice in the presence of obstacles (circles) and exclusion of local interactions (dots).

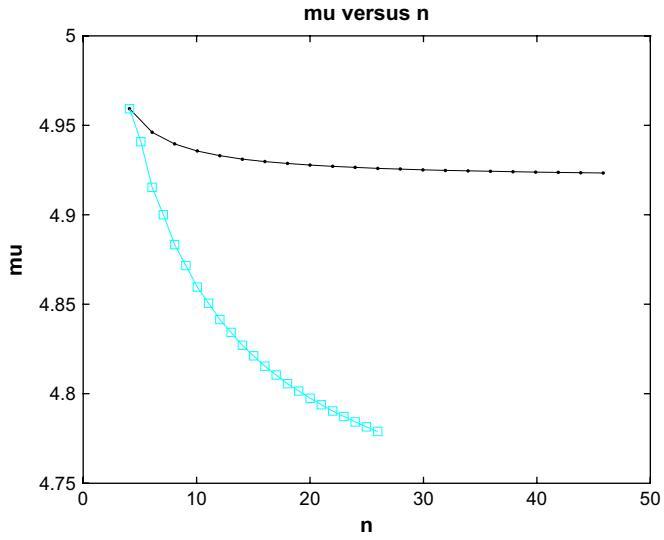

Fig. 16. Comparison of the constant μ as it evolves as the number of segments increases, of the random walk on the cubic lattice when we exclude the local interactions (dots) with the value of μ as found when we take into account the real number of SAWs (squares).

the development of a method that finds upper bounds in combination with an obstacle we did not consider that necessary.

In Fig. 17 we compare $\langle R^8\rangle/\langle R^2\rangle^4$ as they evolve as the number of segments increases, of the random walk on the cubic lattice in the presence of obstacles (circles with thicker line), exclusion of local interactions (dots), and the line derived using the method of Ref. [10] (squares) for calculating the ratios mentioned before for the simple random walk model on the cubic lattice. Since these lines are almost coincident, we notice that the results coincide to the expected values $35/3$ [10–12,20], despite the exclusion of local interactions or the exclusion of walks reaching the obstacles. This means that the values of these

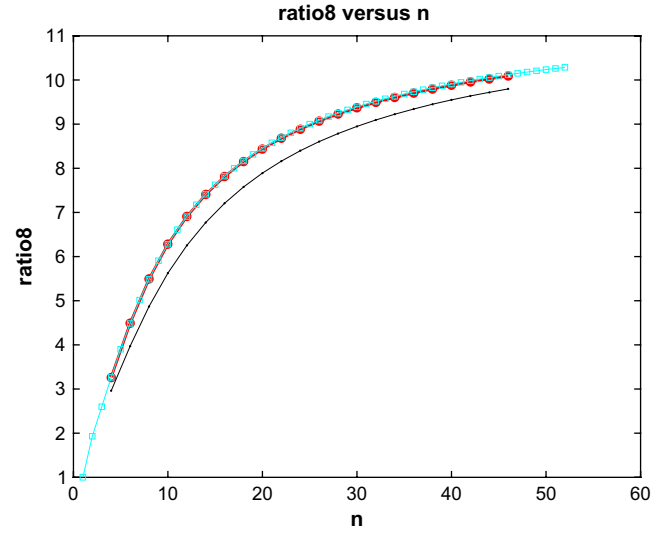

Fig. 17. Ratio8, $\langle R^8\rangle/\langle R^2\rangle^4$, as it evolves as the number of segments increases, of the random walk on the cubic lattice in the presence of obstacles (circles with thicker line), exclusion of local interactions (dots), and the line derived using the method of [10] (squares) for calculating the ratios mentioned before for the simple random walk model on the cubic lattice.

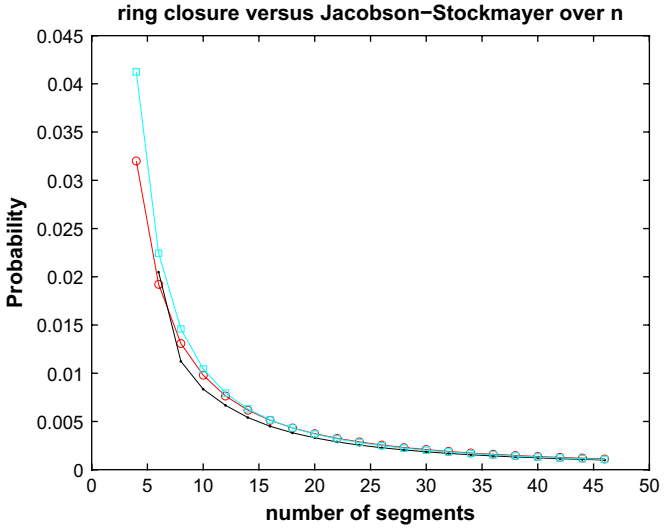

Fig. 18. Comparison of the probability of ring closure (walks terminating at the origin) on the cubic lattice, for the case when we exclude local interactions (dots), when we have obstacles (circles) and we compare it with the classical Jacobson–Stockmayer [9] result (squares) which is given by the formula $P = (3/2\pi n)^{3/2}$ [9].

ratios are not influenced by the presence of obstacles or exclusion of local interactions significantly.

In Fig. 18 we compare the probability of ring closure (walks terminating at the origin) for the case when we exclude local interactions (dots), when we have obstacles (circles) and we compare it with the classical Jacobson–Stockmayer [9] result (squares) which is given by the formula $P = (3/2\pi n)^{3/2}$ [9].

5.4. Tetrahedral lattice

In Fig. 19 we compare the mean end-to-end distance, as it evolves as the number of segments increases, of the random walk on the tetrahedral lattice in the presence of obstacles

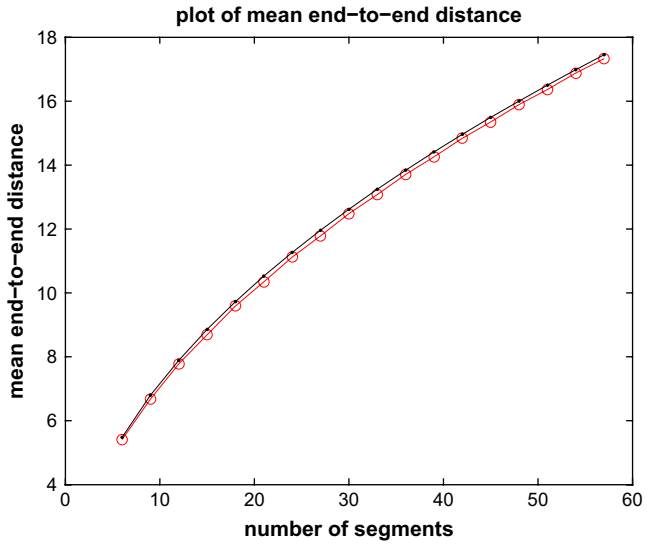

Fig. 19. Comparison of the mean end-to-end distance, as it evolves as the number of segments increases, of the random walk on the tetrahedral lattice in the presence of obstacles (circles), and when we exclude local interactions (dots).

(circles), and when we exclude local interactions (dots). We see that these two lines are almost coincident, and that the value of mean end-to-end distance is around 17.5 at 57 segments.

In Fig. 20 we compare the constant μ as it evolves as the number of segments increases, of the random walk on the tetrahedral lattice when we exclude the local interactions (dots) with the value of μ as found when we take into account the real number of SAWs (squares). We notice that the upper bounds on the connective constant on the tetrahedral lattice are much looser from the real value of μ for the walks that have been counted (up to 30 segments). However, our approximation would improve if we took a greater L. That would require an additional computational cost and since our purpose is to demonstrate the development of a method that finds upper bounds in combination with an obstacle we did not consider that necessary.

In Fig. 21 we compare $\langle R^8\rangle/\langle R^2\rangle^4$ respectively, as it evolves as the number of segments increases, of the random walk on the tetrahedral lattice in the presence of obstacles (circles), exclusion of local interactions (dots), and the line derived using the method of Ref. [10] for calculating the ratios mentioned before (squares) for the simple random walk on the tetrahedral lattice model. Since these lines are almost coincident, we notice that the results coincide to the expected value of $35/3$, [10–12,20], despite the exclusion of local interactions or the exclusion of walks reaching the obstacles. This means that the value of this ratio is not influenced by the presence of obstacles or exclusion of local interactions significantly.

In Fig. 22 we compare the probability of ring closure (walks terminating at the origin) for the case when we exclude local interactions (dots), when we have obstacles (circles) and we compare it with the classical Jacobson–Stockmayer [9] result (squares) which is given by the formula $P = (3/2\pi n)^{3/2}$ [9].

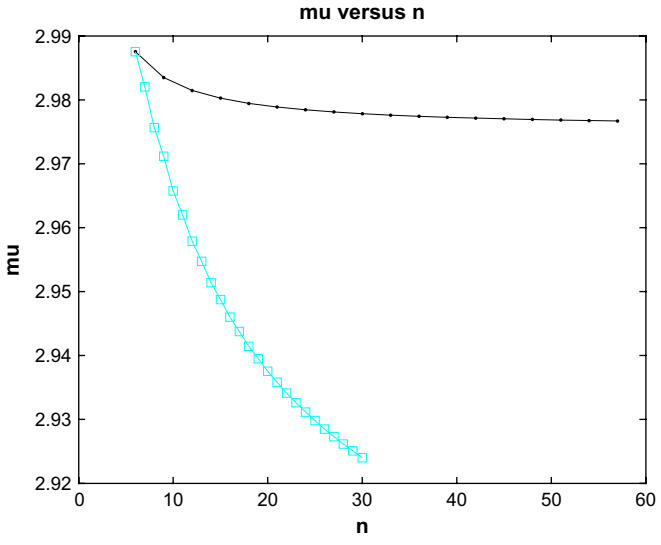

Fig. 20. Comparison of the constant μ as it evolves as the number of segments increases, of the random walk on the tetrahedral lattice when we exclude the local interactions (dots) with the value of μ as found when we take into account the real number of SAWs (squares).

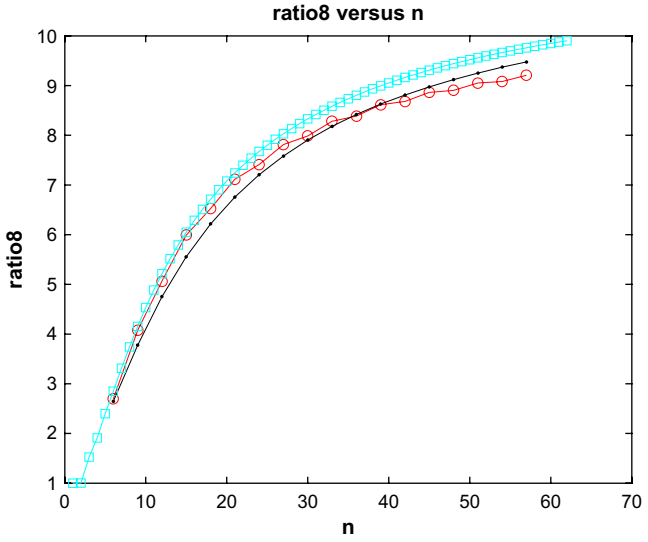

Fig. 21. Ratio8, $\langle R^8\rangle/\langle R^2\rangle^4$, as it evolves as the number of segments increases, of the random walk on the tetrahedral lattice in the presence of obstacles (circles), exclusion of local interactions (dots), and the line derived using the method of Ref. [10] for calculating the ratios mentioned before (squares) for the simple random walk on the tetrahedral lattice model.

5.5. Random walks which are restricted in a small space

Assume the case of the square lattice and assume that the space is constrained from the shape defined by the lines with equations $x = -4$, $y = -4$, $x = 4$, $y = 4$. This means that only the lattice sites that are inside the square created by these lines, that is 49 lattice sites. The way that we deal with this case is the same exactly as described for the case of the obstacle, that is, walks that pass through or attach the border of the obstacle are discarded. We will compare the results of that case with the results that derive from the simple non-reversal random walk case. First of all we will compare μ for both

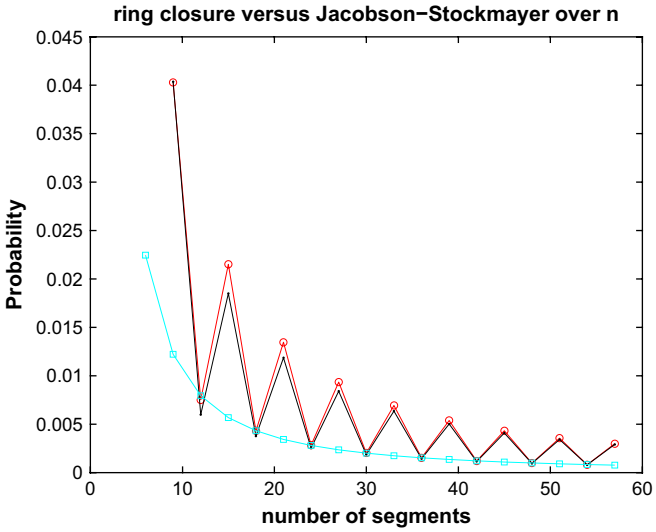

Fig. 22. Comparison of the probability of ring closure on the tetrahedral lattice (walks terminating at the origin) for the case when we exclude local interactions (dots), when we have obstacles (circles) and we compare it with the classical Jacobson–Stockmayer [9] result (squares) which is given by the formula $P = (3/2\pi n)^{3/2}$ [9].

of these cases. In Fig. 23 we see that the number of simple non-reversal random walks on the square lattice (in blue (for interpretation of the reference to colour in text, the reader is referred to the web version of this article)) are always power of 3, whereas those of the constrained space are not. For the 100 segments the number of the walks of the constrained space are 1.1912×10^{42} whereas for the non-reversal random walk the number is 5.1538×10^{47} that is five orders of magnitude more.

Concerning the ring closure (Jacobson–Stockmayer result) we plot the probability of reaching the origin of the constrained walks (in ×s), of the simple non-reversal random walks (in crosses) and of the typical 2-D version of the Jacobson–Stockmayer result (in dots), see Fig. 24. We notice the following: The probability of ring closure for the NRRW using the one-step lattice motion-group convolution and that of the theoretically obtained by the Jacobson–Stockmayer result coincide, whereas that of the constrained space random walk does not converge to the value of the Jacobson–Stockmayer result. That is a surprising discovery because as we saw in the arbitrary obstacle case, the probability of ring closure coincided with of the Jacobson–Stockmayer result. We see what big difference there exists when we restrict the random walk in a confined space compared to the results derived from the existence of a simple obstacle.

5.6. Calculation of entropy and moments

The entropy for each case can be simply found by the formula $S = -K_B \ln(N_T)$, where K_B is the Boltzmann constant and N_T is the total number of random walks that derive from the exclusion of those which pass through the obstacle or those which are locally self intersecting. Concerning the moments, in this paper we calculated the even moments of the mean end-to-end distance. In order to do that we calculated how many times each distance from the origin was reached and then we could easily find the moment of interest by using the formula $\langle R^{2k} \rangle = \sum_i t_i d_i^{2k} / \sum_i t_i$ where t_i is the number of

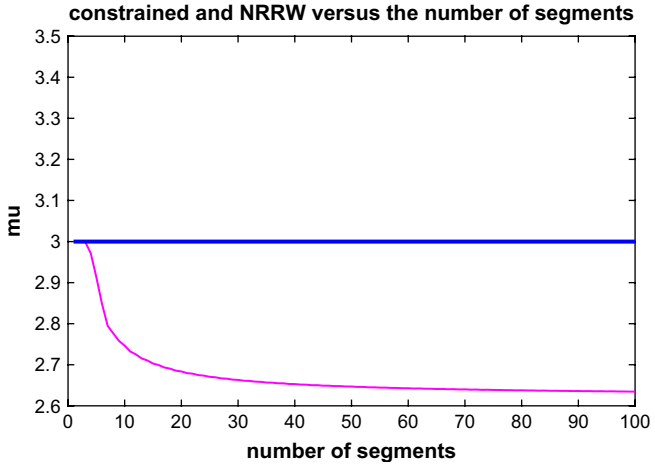

Fig. 23. Comparison of the constant μ of the simple non-reversal random walk on the square lattice (horizontal line) with that of the random walk in the square lattice in a constrained space (curvy decreasing line).

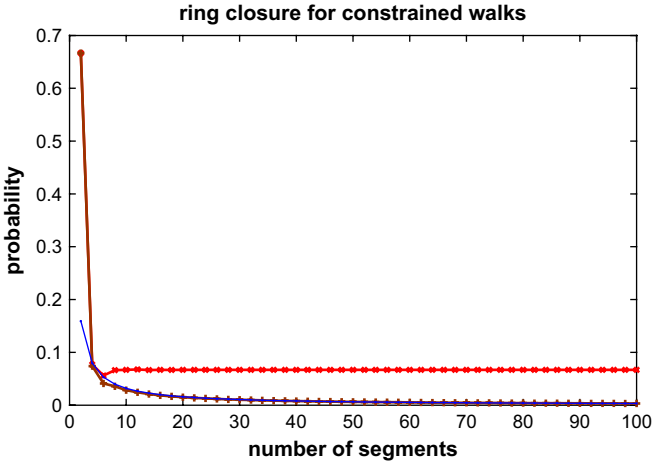

Fig. 24. Comparison of the ring closure probability of the simple non-reversal random walk on the square lattice (crosses) with that of the random walk in the square lattice in a constrained space (×s) and that of the 2-D Jacobson–Stockmayer result (dots).

times each distance is reached, d_i is the particular distance and $\langle R^{2k} \rangle$ is the even moment of the end-to-end distance.

6. Summary

In this paper we presented a novel technique for finding probability distributions for locally self-avoiding walks. In addition to being a more tractable model than globally self-avoiding walks, this model can be used to find bounds on self-avoiding walks in the presence of obstacles, that exclude exactly all the walks that pass through that obstacle. Despite the fact that these bounds are looser, when compared with others developed for SAWs this paper opens a new way to research the area on bounds on SAW's and in the presence of obstacles. The main conclusion is that the selection of the obstacle plays a very big role in the nature of the results. So for each particular obstacle at each particular lattice, we have to examine separately. We cannot describe any analytical way of how the results are modified with the introduction of a new obstacle. We have to apply the method described in the paper and obtain the results numerically, something that this method does fast and accurately.

Acknowledgements

This work was supported under NIH grant R01 GM075310 'Group Theoretic Methods in Protein Structure Determination'.

7. Appendix

7.1. Review of the one-step lattice motion-group convolution

The L-locally self-avoiding walk model builds on our previous work in Ref. [45] on the topic of torsional random walks in which $L = 1$. We therefore review this method here. In order to give a thorough explanation of the one-step lattice motion-group convolution we have first to explain how we treat the

lattice sites and how we use the lattice geometry. The lattices of study are the square, the hexagonal, the cubic and the tetrahedral. The rotational symmetries of these lattices are the symmetries of the corresponding geometric shapes (square, hexagon, cube and tetrahedron, respectively) i.e. the rotations of these shapes that bring them to the same position they were before applying that rotation. To each lattice point now we assign Cartesian coordinates with respect to the lattice point of reference which has lattice coordinates (0,0), or (0,0,0) if it is for 2-D or 3-D lattice, respectively. To that particular lattice site we also assign the particular frame of reference, that is, the directions of the x, y and z axes, respectively. The lattice site that a random walk reaches and the way it reaches it (either from the left or from the right for instance) defines the position of this lattice site with respect to the lattice site of reference and also the orientation with respect to the original frame of reference. The way that a lattice site is reached defines a combination of position and orientation. The same lattice site can be reached by a different way that gives a different combination of position and orientation. This combination of position and orientation can be represented by a 3-*by*-3 or by a 4-*by*-4 matrix depending whether the lattice is 2-D or 3-D and it is explained in text. Let's assume the position and orientation of the end of an N-segment random walk to be

$$g = \begin{pmatrix} A & \mathbf{r} \\ 0^{\mathrm{T}} & 1 \end{pmatrix}. \tag{11}$$

In Fig. 25, we see the original frame of reference e (the identity element) and the end position and orientation of the random walk of N segments g. We see that one way to reach that particular combination of position and orientation g in N segments is

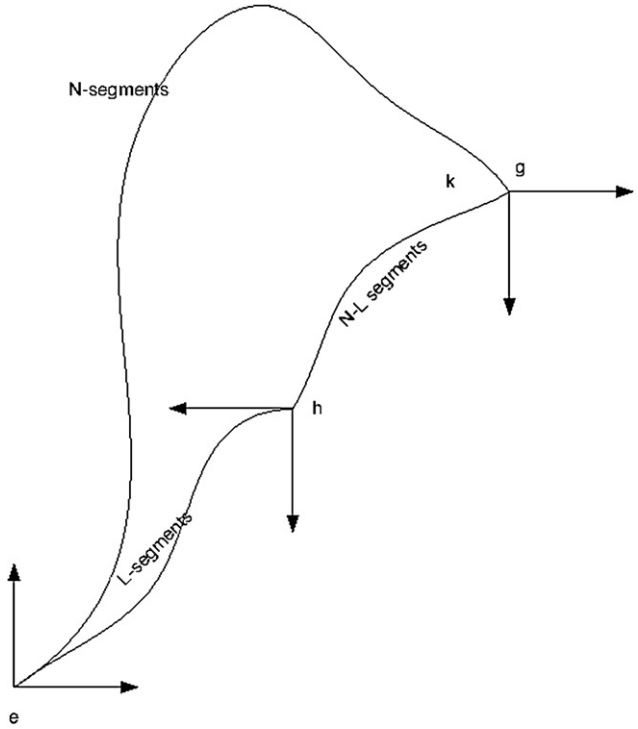

Fig. 25. Explanation of convolution.

to reach at L segments the position and orientation h and at $N-L$ segments the position and orientation k. By concatenating these two positions and orientations we achieve the desired N positions and orientations g for the N segments. This concatenation is mathematically expressed by the matrix multiplication of the matrix representation of h with that of k, that is $h \circ k$. The question that we answer is that given that we know all the end positions and orientations that are reached by the L, and the $N-L$-segment random walk how do we find all the end positions and orientations that are reached by the N-segment random walk. The way we work is simple. For the L-segment random walk we define a function. That function has as input the combination of the end position and orientation and as output the number of times that this combination of position and orientation is reached by the L-segment random walk. Given the fact that the number of different orientations on the lattice is finite and very small (4 for the square, 6 for the hexagonal, 24 for the cubic, 12 for the tetrahedron) we can develop that function very simply by first assigning to each of these discrete rotations − symmetries a symbolic number (that is 1−4 for the square lattice, 1−6 for the hexagonal lattice, 1−24 for the cubic lattice, 1−12 for the tetrahedral lattice). Then we develop a three or four dimensional array (depending on whether the lattice is 2-dimensional or 3-dimensional). The first two (for 2-D lattice) or three dimensions (for 3-D lattice of this array stand simply for the cartesian coordinates of the end lattice site. The last dimension stands for the orientation with which that lattice site is reached. In that particular entry of this array we put the number of times that this particular combination of end position and orientation is reached by the L-segment random walk. The same thing we do for $N-L$-segment random walk. So in order to find how many times a combination of end position and orientation is reached by the N-segment random walk we calculate the sum

$$f_N(g) = \sum_h f_L(h) f_{N-L}(k) = \sum_h f_L(h) f_{N-L}\left(h^{-1} \circ g\right). \tag{12}$$

What this equation says is simply that in order to calculate how many times that particular combination of position and orientation is reached by the N-segment random walk you calculate for each position and orientation h that is reached by the L-segment random walk the real number product $f_L(h) f_{N-L}(h^{-1} \circ g)$, and then we sum over all h. The conception is very logical because you have to multiply $h^{-1} \circ g$ on the right of h in order to get g. We directly know how many walks of length N that at the Lth segment terminate at the h position and orientation, terminate at the g position and orientation at the Nth segment. If $L = 1$ then we have the one-step lattice motion-group convolution.

References

[1] Pappu RV, Srinivasan R, Rose GD. The Flory isolated-pair hypothesis is not valid for polypeptide chains: implications for polypeptide unfolded states. Proceedings of the National Academy of Sciences USA 2000;97:12565–71.

[2] Chirikjian GS. Conformational statistics of macromolecules using generalized convolution. Computational Theoretical Polymer Science February 2001;11:143–53.
[3] Alexandrowicz Z. Monte Carlo of chains with excluded volume – a way to evade sample attrition. Journal of Chemical Physics 1969;51:561–5.
[4] Hiller A, Wall FT, Wheeler DJ. Statistical computation of mean dimensions of macromolecules. Journal of Chemical Physics 1954;22:1036.
[5] Wall WA, Seitz FT. Simulation of polymers by self-avoiding non intersecting random chains at various concentrations. Journal of Chemical Physics 1977;67:3722–6.
[6] Alexandrowicz Z, Accad Y. Monte Carlo of chains with excluded volume: distribution of intersegmental distances. Journal of Chemical Physics 1971;54:5338–45.
[7] Kremer K, Binder K. Monte Carlo simulations of lattice models for macromolecules. Computer Physics Reports 1988;7:259–310.
[8] Sokal AD. Monte Carlo methods for the self-avoiding walk. Monte Carlo and molecular dynamics simulations in polymer science. New York, NY: Oxford University Press; 1995.
[9] Jacobson H, Stockmayer WH. Intramolecular reaction polycondensations. I. The theory of linear systems. Journal of Chemical Physics 1950;18(12):1600–6.
[10] Mattice WL, Sienicki K. Extent of the correlation between the squared radius of gyration and squared end-to-end distance in random flight chains. Journal of Chemical Physics 1989;90(3):1956–9.
[11] Flory PJ, Jernigan RL. Second and fourth moments of chain molecules. Journal of Chemical Physics 1965;42(10):3509–19.
[12] Jernigan RL, Flory PJ. Moments of chain vectors for models of polymer chains. Journal of Chemical Physics 1969;50(10):4178–85.
[13] Madras N, Slade G. The self avoiding walk. Boston, MA: Birkhauser; 1993.
[14] Crippen GM. Enumeration of cubic lattice walks by contact class. Journal of Chemical Physics 2000;112:11065.
[15] Kloczkowski A, Jernigan RL. Transfer matrix method for enumeration ansi generation of compact self-avoiding walks. 1. Square lattices. Journal of Chemical Physics 22 September 1998;109(12):5134–46.
[16] Kloczkowski A, Jernigan RL. Transfer matrix method for enumeration and generation of compact self-avoiding walks. II. Cubic lattice. Journal of Chemical Physics 22 September 1998;109(12):5147–59.
[17] Kloczkowski A, Jernigan RL. Computer generation and enumeration of compact self-avoiding walks within simple geometries on lattices. Computational and Theoretical Polymer Science 1997;7(3–4):163–73. Part 1.
[18] Caracciolo S, Guttmann AJ, Jensen I, Pelissetto A, Rogers AN, Sokal AD. Correction-to-scaling exponents for two-dimensional self-avoiding walks. Journal of Statistical Physics September 2005; 120(5–6):1037–100.
[19] MacDonald D, Joseph S, Hunter DL, Moseley LL, Jan N, Guttmann AJ. Self avoiding walks on the simple cubic lattice. Journal of Physics A: Mathematical and General 2000;33:5973–83.
[20] Kotelyanskii M, Theodorou DN. Simulation methods for polymers. New York, NY: Marcel Dekker Inc; 2004.
[21] Metropolis N, Rosenbluth AW, Rosenbluth MN, Teller AH, Teller E. Equation of state calculations by fast computing machines. Journal of Chemical Physics 1953;21:1087–92.
[22] Adler J. The self-avoiding walk on the honeycomb lattice. Journal of Physics A: Mathematical and General 1983;16:L515–7.
[23] Casassa EF. Polymer solutions. Annual Reviews of Physical Chemistry 1960;11:477–500.
[24] Chay TR. Distribution function for self avoiding walks. Journal of Chemical Physics 1971;52:1025–33.
[25] Chay TR. Distribution function for self-avoiding walks. II. Numerical part. Journal of Chemical Physics 1972;57:910–2.
[26] Conway AR, Guttmann AJ. Enumeration of self avoiding trails on a square lattice using a transfer matrix technique. Journal of Physics A: Mathematical and General 1993;26:1535–52.
[27] Conway AR, Enting IG, Guttmann AJ. Algebraic techniques for enumerating self-avoiding walks on the square lattice. Journal of Physics A: Mathematical and General 1993;26:1519–34.
[28] de Gennes P-G. Reptation of a polymer chain in the presence of fixed obstacles. Journal of Chemical Physics 1971;55:572–9.
[29] Domb C. Self-avoiding walks on lattices. Advances in Chemical Physics 1969;15:229–59.
[30] Domb C. From random to self-avoiding walks. Journal of Statistical Physics 1983;30:425–36.
[31] Lin KY, Lee FY, Chen CN, Chao NC. Position-space renormalization group for SAWs on the L lattice. Journal of Physics A: Mathematical and General 1990;23:601–4.
[32] MacDonald D, Hunter DL, Kelly K, Jan N. Self-avoiding walk in two to five dimensions. Exact enumerations and series study. Journal of Physics A: Mathematical and General 1992;25:1429–40.
[33] Mark P, Windwer S. Self-avoiding walks on the tetrahedral lattice. Journal of Chemical Physics 1967;47:708–10.
[34] Martin JL. The exact enumeration of self-avoiding walks on a lattice. Proceedings of the Cambridge Philosophical Society 1962;58:92–101.
[35] Martin JL, Watts MG. The end-point distribution of self-avoiding walks. Journal of Physics A: Mathematical and General 1971;4:456–63.
[36] McKenzie DS. The end-to-end length distribution of self-avoiding walks. Journal of Physics A: Mathematical and General 1973;6:338–52.
[37] Moon J, Nakanishi H. Self-avoiding Levy walk: a model for stiff polymers. Physical Review A 1990;42:3221–4.
[38] Morita T. A lattice model for a polymer chain in dilute solution. Journal of Physics A: Mathematical and General 1976;9:169–77.
[39] Nemirovsky AM, Freed KF, Ishinabe T, Douglas JF. End-to-end distance of a single self-avoiding polymer chain: d^{-1} expansion. Physics Letters 1992;162A:469–74.
[40] Wall FT, Hiller LA. Properties of macromolecules in solution. Annual Review of Physical Chemistry 1954;5:267–91.
[41] Wall FT, Hioe FT. The distribution of end-to-end lengths of self-avoiding walks on the diamond lattice. Journal of Physical Chemistry 1970;74: 4410–5.
[42] Watts MG. The end-point distribution of self-avoiding walks on a crystal lattice II. Loose-packed lattices. Journal of Physics A: Mathematical and General 1974;8:489–94.
[43] Summers DW, Whittington SG. Knots in self-avoiding walks. Journal of Physics A: Mathematical and General 1988;21:1689–94.
[44] Sykes MF. Self-avoiding walks on the simple cubic lattice. Journal of Chemical Physics 1963;39:410–2.
[45] Skliros A, Chirikjian GS. Torsional random walk statistics on lattices using convolution on crystallographic motion groups. Polymer 2007;48:2155–73.
[46] Alm SE, Parviainen R. Bounds for the connective constant of the tetragonal lattice. Journal of Physics A: Mathematical and General 2004;37: 549–60.
[47] Chen M, Lin KY. Universal amplitude ratios for three-dimensional self-avoiding walks. Journal of Physics A: Mathematical and General 2002; 35:1501–8.
[48] Faulon JL, Rintoul MD, Young MM. Constrained walks and self-avoiding walks: implications for protein structure determination. Journal of Physics A: Mathematical and General 2002;35:1–19.
[49] Ishinabe T. Critical exponents for surface interacting self-avoiding walks.III. Infinite systems. Journal of Chemical Physics 1984;80(3):1318–25.
[50] Jensen I. Enumeration of self-avoiding walks on the square lattice. Journal of Physics A: Mathematical and General 2004;37:5503–24.
[51] Middlemiss KM, Whitington SG. Exact enumeration of self-avoiding walks on the cubic lattice terminally attached to an interface. Journal of Chemical Physics 1976;64(11):4684–8.
[52] Wall FT, White RA. Macromolecular configurations simulated by random walks with limited orders of non-self-intersection. Journal of Chemical Physics 1976;65(2):808–12.
[53] Kloczkowski A, Jernigan RL. Efficient method to count and generate compact protein lattice conformations. Macromolecules 1997;30:6691–4.
[54] Bennett-Wood D, Owczarek AL. Exact enumeration for self-avoiding walks on the honeycomb lattice attached to a surface. Journal of Physics A: Mathematical and General 1996;29:4755–68.
[55] Jensen I. Improved lower bounds on the connective constants for two-dimensional self-avoiding walks. Journal of Physics A: Mathematical and General 2004;37:11521–9.

[56] Noonan J. New upper bounds for the connective constants of self-avoiding walks. Journal of Statistical Physics 1998;91(5/6).
[57] Guttmann AJ. Bounds on connective constant for self-avoiding walks. Journal of Physics A: Mathematical and General 1983;16:2233–8.
[58] Mattice WL, Suter UW. Conformational theory of large molecules: the rotational isomeric state in macromolecular systems. New York, NY: Wiley; 1994.
[59] Mark JE, Abou-Hussein R, Sen TZ, Kloczkowski A. Some simulations on filler reinforcement in elastomers. Polymer 2005;46:8894–904.
[60] Sharaf MA, Mark JE. Monte Carlo simulations on the effects of nanoparticles on chain deformations and reinforcement in amorphous polyethylene networks. Polymer 2004;45:3943–52.
[61] http://www.hermetic.ch/compsci/lattgeom.htm.